



HAL
open science

Healing Near-PT-Symmetric Structures to Restore Their Characteristic Singularities: Analysis and Examples

Henri Benisty, Chen Yan, Aloyse Degiron, Anatole Lupu

► **To cite this version:**

Henri Benisty, Chen Yan, Aloyse Degiron, Anatole Lupu. Healing Near-PT-Symmetric Structures to Restore Their Characteristic Singularities: Analysis and Examples. *Journal of Lightwave Technology*, 2012, 30 (16), pp.2675. 10.1109/JLT.2012.2205222 . hal-00818846

HAL Id: hal-00818846

<https://hal-iogs.archives-ouvertes.fr/hal-00818846>

Submitted on 26 Aug 2022

HAL is a multi-disciplinary open access archive for the deposit and dissemination of scientific research documents, whether they are published or not. The documents may come from teaching and research institutions in France or abroad, or from public or private research centers.

L'archive ouverte pluridisciplinaire **HAL**, est destinée au dépôt et à la diffusion de documents scientifiques de niveau recherche, publiés ou non, émanant des établissements d'enseignement et de recherche français ou étrangers, des laboratoires publics ou privés.

Healing Near-PT-Symmetric Structures to Restore Their Characteristic Singularities: Analysis and Examples

Henri Benisty, *Member, IEEE*, Chen Yan, Aloyse Degiron, and Anatole T. Lupu

Abstract—PT-symmetric structures, such as a pair of coupled waveguides with balanced loss/gain, exhibit a singularity of their eigenvalues around an exceptional point, hence a large apparent differential gain. In the case of fixed losses and variable gain, typical of plasmonic systems, a similar behavior emerges but the singularity is smoothed, especially in more confined structures. This reduces the differential gain around the singular point. Our analysis ascribes the origin of this behavior to a complex coupling between the waveguides once gain is present in an unsymmetrical fashion, even if guides feature the same modal gains in isolation. We demonstrate that adjunction of a real index variation to the variable waveguide heals the singularity nearly perfectly, as it restores real coupling. We illustrate the success of the approach with two geometries, planar or channel, and with different underlying physics, namely dielectric or plasmonic.

Index Terms—Integrated optoelectronics, optical amplifiers, waveguides, coupled mode analysis.

I. INTRODUCTION

RECENTLY, a great interest has been paid to the unusual properties of PT-symmetric structures, that is structures where gain and loss are exchanged by a mirror symmetry [1]–[4]. One “flavor” under which such PT symmetry comes uses a plane of symmetry normal to a waveguide, but it then demands a specific periodic pattern of gain and real index perturbations [5]–[7]. The other “flavor” considers two waveguides with initially identical modal (effective) index $n_{\text{eff},1} = n_{\text{eff},2}$ [2], [8]–[11]. We prefer here this second version, which is also more prone to possible implementation in switching devices. When gain is increased in one of the coupled waveguides and losses are symmetrically adjusted in the other, an exceptional point arises in the behavior of the eigenvalues [2], [4], [12], [13]. The eigenvalues that were both real below this exceptional point (in spite of gain in the system) become complex conjugate beyond.

At or around such an exceptional point, the output has a very large swing if the material gain is changed only by a small

amount and if the length of the device is long enough, meaning in other words that there is a large differential gain in the system. We invoked this in our recent contributions on PT symmetry with plasmonic systems [12], [14]. Because of the limited extent of this interesting regime, the device useful operation range, i.e., with both substantial gain and high differential gain, has to be assessed. We will first do such an assessment, resulting in a simple specification for device length and a framework for our subsequent results.

What we mainly wish to address here is the restoration of a near-perfect singularity in practical cases of interest where it tends to be smoothed. The smoothing phenomenon is general: if one starts from identical waveguides at zero gain/zero loss, modifying their material constant to bring gain to one of them and loss to the other impacts not only the real part of the propagation constant, but also the coupling constant, which tends to become intrinsically complex. The smoothing of the singularity by a complex coupling constant, thus, has to be mastered for the rest of the study.

Two reasons have also attracted us toward attempts of PT-symmetry operation with fixed losses instead of variable ones: first the impracticality to impose balanced losses and gain, and second and most important, the advent of plasmonic gain/laser structures [15]–[17], so-called spasers [18] for instance, whereby a fixed loss imparted by the metal contribution, which is rather large in basic plasmonic waveguide designs in the infrared to visible ranges, is decently mitigated by solutions such as the “hybrid plasmonic waveguides” [19], [20]. Such reduced losses can, therefore, be realistically balanced by gain from known materials systems, be it in organics-based or in semiconductor-based structures.

We also argued in [14] that in the case of fixed losses + variable gain, corresponding to the much investigated case of active plasmonics, one can get a similar PT-symmetric system with still an exceptional point in the eigenvalue evolution, at least in a basic model, provided that coupling is adjusted between the first gain-carrying waveguide and the second, fixed-loss waveguide. In brief, since the exceptional point occurs when gain and coupling critically compete, adjusting the coupling to the critical value dictated by the fixed losses in the second waveguide does result in an exceptional point singularity similar in most respects to the balanced case. The singularity then occurs at the gain value opposite to the fixed losses [14].

When turning to real systems with standard electromagnetic description, the applicability of coupled-mode theory requires arrangements, targeting, as said previously, the complex nature

H. Benisty and C. Yan are with Laboratoire Charles Fabry, Institut d’Optique, CNRS, Univ Paris Sud, 2, Avenue Augustin Fresnel, 91127 Palaiseau Cedex, France (e-mail: henri.benisty@institutoptique.fr; ycrichard330@gmail.com).

A. Degiron and A. T. Lupu are with the Institut d’Electronique Fondamentale, UMR 8622 du CNRS, Univ ParisSud, 91405 Orsay Cedex, France (e-mail: aloyse.degiron@ief.u-psud.fr; anatole.lupu@ief.u-psud.fr).

of the coupling constant. For instance, we substantiated the finding of coupled-mode theory with two calculations either on 1-D waveguide models or on long-range surface plasmon polariton (LRSPP) waveguides [21] two cases rather corresponding to “deconfined” modal strategies. In both of them, the singularity was very well restored, albeit not to mathematical perfection. Unfortunately, when we considered more confined waveguides such as the PIROW waveguide [12], [22], we observed that the singularity could be substantially washed out, even if gain and coupling were adjusted together.

This can be understood because the addition of the same amount of gain or loss to lossless waveguides affects the coupling coefficient with the other guide. Even if two guides have equal modal gains/losses when considered in isolation, we will see for instance that because of the repartition of gain and loss in each of them, a relevant coupling coefficient product is no more purely real.

The scope of this paper is therefore, after the assessment of differential gain mentioned previously, to present an analysis and a strategy to restore a more spiked exceptional point behavior in spite of the adverse effects observed in real structures, that is “healing” the smoothing of the singularity. For this, we first infer the complex coupling coefficients from the exact calculation and deduce how they should be modified. The modification is targeted at compensating the imaginary part of the coupling to restore a real coupling. This strategy, therefore, amounts to modify continuously the real part of the dielectric constants in adequate proportion with the variation of gain, to get from the optogeometric parameters a proper coupled-mode equivalent behavior. We gave a first example of this in [12]. As is intuitive from this strategy, if the imaginary part to be compensated is modest, the amount of real part of the dielectric constant to be modified will be also modest in comparison to the gain (imaginary part) variation, which makes the approach sensible.

In Section II, we give the assessment of “PT-symmetry enhanced” differential gain. We introduce a phenomenological phase in the coupling constant and observe how it degrades and dilutes the singularity. In Section III, we give the analysis of the complex coupling in such a way that the remedying strategy is logically deduced in terms of rotation in a representative complex plane and more usefully in terms of detuning. In Section IV, we present first simple numerical examples, based on a pair of waveguides which are modified in such a way as to explicitly adjust the complex coupling constant while operating at a nearly fixed effective index. We next apply our method to a more realistic case and heal the singularity as well. Slab and channel geometries are exemplified, with, in the latter case, either a pair of “PIROW” inverse-rib hybrid plasmonic waveguides [12], [22] or the LRSPP [14], [21] as the loss-carrying waveguide.

II. PT COUPLED MODE THEORY, SINGULARITY AND DIFFERENTIAL GAIN ENHANCEMENT

In its generic version, a PT-symmetric system of two waveguides [see Fig. 1(a)] can be modeled by the matrix coupled wave equation

$$i \frac{d}{dz} \begin{bmatrix} \psi_1 \\ \psi_2 \end{bmatrix} = M \begin{bmatrix} \psi_1 \\ \psi_2 \end{bmatrix} \quad (1)$$

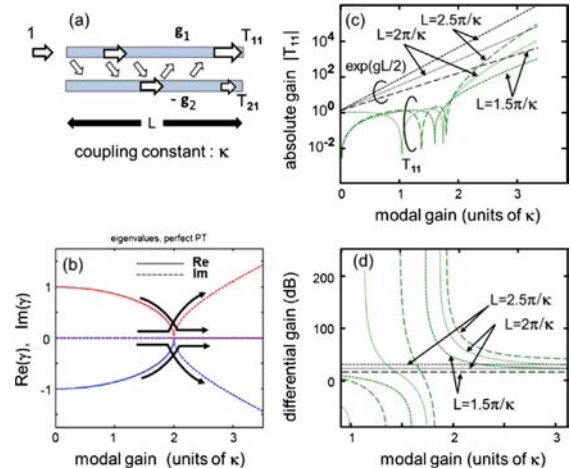


Fig. 1. Two coupled waveguides with perfect PT-symmetry and no complex coupling: (a) coupled waveguides and definition of main quantities; (b) eigenvalues real and imaginary parts versus normalized modal gain g/κ ; (c) absolute amplitude gain of the device in the “bar” configuration for lengths $L\kappa/\pi = 1.5, 2.0$, and 2.5 (curves as indicated), as a function of normalized modal gain g and comparison with isolated waveguide gain $\exp(gL/2)$; (d) differential gain in dB per normalized gain unit $[d(20 \log_{10}(T_{11}))/d(g/\kappa)]$ for the three cases of (c): $L\kappa/\pi = 1.5$ (short dashed line), $L\kappa/\pi = 2.0$ (dotted line), $L\kappa/\pi = 2.5$ (long dashed line). The horizontal lines show the constant differential gain of the isolated gain-carrying waveguide, proportional to L .

where $\psi_1(z)$ and $\psi_2(z)$ are the amplitudes of the two waveguide modes, and the matrix M is

$$M = \begin{bmatrix} m_{11} & m_{12} \\ m_{21} & m_{22} \end{bmatrix} = \begin{bmatrix} \tilde{\beta}_1 & \tilde{\kappa}_1 \\ \tilde{\kappa}_2 & \beta_2 \end{bmatrix} = \begin{bmatrix} \beta_1 + ig_1/2 & \tilde{\kappa}_1 \\ \tilde{\kappa}_2 & \beta_2 - ig_2/2 \end{bmatrix} \quad (2)$$

where the individual mode’s propagation constants $\tilde{\beta}_j$ include gain $g_1 > 0$ and loss: with our convention losses are described by $g_2 > 0$ as well. The coupling constants $\tilde{\kappa}_1, \tilde{\kappa}_2$ are in general complex. In a perfect coupling case, we assume that $\beta_1 = \beta_2$; in other words, the so-called detuning $\delta = \beta_2 - \beta_1$ is zero, and phases are matched between the two passive modes (this will not be the case in next sections where a role of δ will emerge).

If $g_1 = g_2 = g$ and $\tilde{\kappa}_1, \tilde{\kappa}_2$ are real valued and identical, then varying the value of g , and looking at the eigenvalues γ_j of M , see Fig. 1(b), we have a perfect singularity [2], [4] at the exceptional point $g_c = 2\kappa$, that is a critical gain value that exactly coincides with the eigenvalues splitting at $g = 0$, $\Delta\gamma = 2\kappa$. Thus, we make use in the following of the normalized gain g/κ as the abscissa. Of course, the imaginary part of the propagation eigenvalues γ_1, γ_2 is exactly zero in this case at the exceptional point. The singularity at the exceptional point means that eigenvalues evolve locally faster, and quadratically, with the underlying modal gain (or bulk gain) and loss of the isolated waveguides.

The transmission matrix T of a device of length L is easily calculated according to $T = P \exp(DL)P^{-1}$, where D is the diagonal matrix composed of the $-iM$ eigenvalues $D_{jj} = \gamma_j$ and P is the matrix of the eigenvectors of $-iM$. We show in the semilog plot of Fig. 1(c) the resulting “bar” transmission $T_{11}(g)$, compared to the case of plain amplitude amplification $\exp(gL/2)$. While gain is obviously lower due to the coupling,

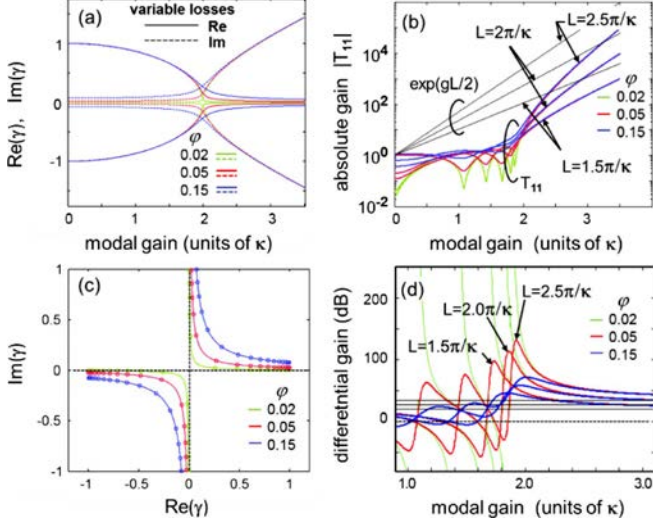


Fig. 2. Perfect PT symmetry, i.e., balanced gain and losses, with variable degrees of complex coupling, $\varphi = 0.02, 0.05$, and 0.15 (the coupling constant product is $\tilde{\kappa}_1 \tilde{\kappa}_2 = e^{i\varphi}$); (a) real and imaginary parts as a function of modal gain g ; (b) gain of the coupled system for different lengths L for the three phases, showing the smoothing of the high slope region around $g = 2$, the straight lines being $\exp(gL/2)$; (c) eigenvalues trajectories in complex plane, with dots associated with linearly spaced gain values; (d) differential gain for different lengths and phases as in (b); the horizontal solid lines show the constant differential gains of isolated gain-carrying waveguides.

there is an abrupt change from $|T_{11}| = 0$ to $|T_{11}| \gg 1$ close to the exceptional point. Fig. 1(c) shows that this rapid transition holds best for the longest waveguides and occurs closer and closer to the exceptional point as the device length increases. This behavior has already been evidenced in [14, Fig. 1] and mostly results from a change in the way the waveguides interact below and above the exceptional point. Just below the exceptional point, we have $|T_{11}| = 0$ because the length of the device is such that all the signal is coupled to the lossy waveguide. Above the exceptional point, the signal propagating in a PT-symmetric structure is always transmitted through the gain channel, leading to a strong overall gain $|T_{11}| \gg 1$ if the device is sufficiently long. In other words, we have a reasonably narrow region around the exceptional point where a change in the coupling properties produces a feature that cannot be afforded by a single guide, and consequently genuinely offers a novel device opportunity.

The abrupt changes in $|T_{11}|$ for the three lengths considered here imply that the differential gain is very high in the vicinity of the exceptional point. This is best seen in Fig. 1(d) which gives a plot of the “PT-enhanced” differential gain enhancement.

Next, playing with this model, we can readily address in a general manner the effect of a *complex* coupling constant. More precisely, we can take constants with a complex product such as $\tilde{\kappa}_1 = \tilde{\kappa}_2 = \kappa e^{i\varphi/2}$. The eigenvalues γ_j are determined by the product $\tilde{\kappa}_1 \tilde{\kappa}_2 = e^{i\varphi}$. We use this phase φ of the product as a parameter, in Fig. 2(a), (b), and (d) which complements Fig. 1(b)–(d) for three different phases φ . In Fig. 2(c), we have added a complex plane representation of the eigenvalue trajectories, showing how the phase causes the poles trajectories to repel. It is obvious that a complex constant tends to wash out the singularity, but the enhanced differential gain is still robust

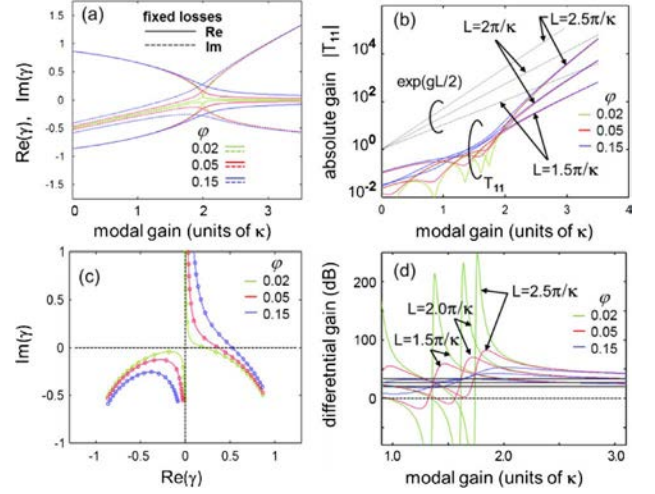


Fig. 3. Imperfect PT symmetry with constant losses, and with variable degrees of complex coupling, $\varphi = 0.02, 0.05$, and 0.15 ; (a) real and imaginary parts as a function of modal gain g ; (b) gain of the coupled system for different lengths L for the three phases, showing the smoothing of the high slope region around $g = 2$, the straight lines being $\exp(gL/2)$; (c) eigenvalues trajectories in complex plane, with dots associated with linearly spaced gain values: at zero gain, loss dominates (negative $\text{Im}(\gamma)$ for both branches); (d) differential gain for different lengths and phases as in (b); the horizontal solid lines show the constant differential gains of isolated gain-carrying waveguides.

against this adverse effect up to phase values of about 0.1. It actually avoids differential gain peaking. We will see later in more detail how real systems correspond to this situation.

Furthermore, we can consider still in a general manner the fixed loss condition that we discussed in [14]: it is the reference situation for the use of plasmonics for wave-guiding. It is indeed interesting to combine gain and losses not just to fight losses of plasmonic waveguides, but to fruit the possibility of “PT-enhanced differential gain” discussed previously. We, thus, have

$$M = \begin{bmatrix} \beta_1 + ig/2 & \tilde{\kappa}_1 \\ \tilde{\kappa}_2 & \beta_2 - ig_0/2 \end{bmatrix}. \quad (3)$$

As explained in [14], to maintain the singularity/degeneracy at the same central eigenvalue position ($\gamma_j = 0$), the fixed losses (in amplitude) and coupling constant should be matched, $\kappa = g_0/2 \equiv g_2/2$, and the singularity occurs when the variable gain $g \equiv g_1$ also matches 2κ . In Fig. 3(a)–(d), we, therefore, do the same exercise as in Fig. 2(a)–(c) but for this fixed loss situation. It is clear that there is a price to pay and that the differential gain enhancement is reduced. But in essence the phenomenology is conserved and the combination produces substantially more differential gain in an acceptable range of the variable gain and of the variable phase of the coupling coefficient.

With all these elements in mind (perfect case, Fig. 1, role of phase, Fig. 2, and situation of fixed losses, Fig. 3), we can now proceed and explain in the next section how one can heal a given real system. The difference is that in a real system, the eigenvalue pattern is not found by diagonalizing a matrix, but by an exact electromagnetic calculation (1-D for coupled slab modes or 2-D for coupled channel modes). Therefore, the handles are not direct, and more understanding has to be provided to manipulate those handles. We stick to the case of fixed losses because

we believe it is more realistic. We, thus, study how the degradation in differential gain enhancement due to complex coupling can be mitigated.

III. HEALING IMPERFECT PT SYMMETRY: COUPLED MODE APPROACH TO PREDICT DETUNING

We now turn to the converse issue of “healing” an imperfect PT-symmetry exceptional point, and we concentrate on the fixed loss cases. We first manipulate the CMT model in such a way that its parameters can be retrieved from the sole evolution of eigenvalue versus g . This is because, for exact systems modeled in 1-D or 2-D, the coupling coefficient can be tricky to safely determine, whereas there is generally no doubt on the eigenvalue spectrum evolution. Such a spectrum could stem for instance from a mode solver, and is generally reliable.

In general, the product of the two coupling coefficient is complex $\tilde{\kappa}_1 \tilde{\kappa}_2 = K e^{i\varphi}$ (with K and φ real). The physical reason for a complex valued product starts by remarking that the two terms $\tilde{\kappa}_1$ and $\tilde{\kappa}_2$ are independent. They are related to the overlap of one mode’s tail to the other guide’s gain or loss region. For instance, these active regions may be positioned in arbitrary regions within the respective guides provided that integrated other their own mode profile, each achieves the given gain g or loss g_0 . Formally, imagine a slab waveguide with gain in only one half of it. This half can be either close or far from the other waveguide; nevertheless, the modal gain of the isolated waveguide would be the same, whereas the overlap integral would differ since gain would be further in the tail in the “far” case. More generally, because there is no *a priori* relation between the two modes (core or tail), the two overlaps may take distinct complex values, preventing the coupling constant product to be real.

Solving the eigenvalues γ_{\pm} of matrix M by requesting $\det(M - \gamma I) = 0$ yields a second-order equation $\gamma^2 - (m_{11} + m_{22})\gamma + \det(M) = 0$, whose roots can be written, with easy algebra:

$$\gamma = \gamma_{\pm} = \frac{1}{2} \left(m_{11} + m_{22} \pm [(m_{11} - m_{22})^2 + 4m_{12}m_{21}]^{1/2} \right). \quad (4)$$

The discriminant $\Delta = (m_{11} - m_{22})^2 + 4m_{12}m_{21}$ is independent of the absolute index (similarly to the fact that there is no energy origin in quantum mechanics, the splitting is independent of the mean effective index of these diagonal elements). Some more algebra on the detailed form of M gives

$$\Delta = -\frac{1}{4}[2i\delta - (g_0 + g)]^2 + 4K e^{i\varphi} \quad (5)$$

whereby only the detuning $\delta = \beta_2 - \beta_1$ appears, not the absolute indices. This has an interesting consequence: if we start from only the knowledge of the two eigenvalues γ_+, γ_- (e.g., they are complex effective indices n_{eff} obtained from a mode solver in a simulation), we have from (4) $(\gamma_+ - \gamma_-) = \sqrt{\Delta}$; thus, $(\gamma_+ - \gamma_-)^2 = \Delta$. By separating the real and imaginary parts in the difference $R + iC = (\gamma_+ - \gamma_-)$, we get from (5) two identities

$$R^2 - C^2 = -\frac{1}{4}(g_0 + g)^2 + \delta^2 + 4K \cos \varphi \quad (6)$$

$$2RC = \delta(g_0 + g) + 4K \sin \varphi. \quad (7)$$

Thus, eliminating K , we can retrieve φ for *any* starting data

$$\tan \varphi = \frac{2RC - \delta(g_0 + g)}{R^2 - C^2 - \delta^2 + \left(\frac{1}{4}\right)(g_0 + g)^2}. \quad (8)$$

This is an important piece as it shows that the coupling product phase φ (and then K) can be retrieved from the combined knowledge of *the sole eigenvalue difference of the coupled guides* and the gain/loss and detuning of the isolated guides (three parameters). Note that the formal signs attributed to the two eigenvalues do not matter in (8).

By the same token, we have gained a useful approach to heal systems with imperfect PT symmetry due to complex coupling, and which are characterized by a large nonzero lower bound for the eigenvalue “distance” in a complex plane $|\gamma_+ - \gamma_-| > |\gamma_+ - \gamma_-|_{\text{min}}$, as observed in Section II models and in reality. Since the optimal PT-symmetry-related singularity is characterized by a root degeneracy, see Fig. 1(a), we want to force a point such that $(\gamma_+ - \gamma_-) = \sqrt{\Delta} = 0$ at the singular point and we will do that by adjusting the detuning parameter $\delta = \beta_2 - \beta_1$ first from an algebraic point of view, and second with a graphical justification.

We take the freedom to add the condition $\text{Im}(\gamma_+) = \text{Im}(\gamma_-) = 0$ at the *singular point* which anyway verifies $\gamma_+ = \gamma_-$: it is reasonable to take advantage of a high differential gain in a region where the gain is not smaller than unity, nor too much higher. This greatly simplifies the final expressions without sacrificing the principle. Since in the case $\Delta = 0$, the roots are $(1/2)(m_{11} + m_{22})$ and their imaginary part is $i((g_0 - g)/(4))$, we, thus, request $g = g_0$ at the *singular point*. Now (5) greatly simplifies and $\Delta = 0$ reads

$$(i\delta - g_0)^2 = 4K e^{i\varphi}. \quad (9)$$

We now get a complex equation whose real and imaginary parts finally provide the optimized values of \sqrt{K} and δ as follows:

$$g_0 - i\delta = 2\sqrt{K} e^{i\varphi/2} \quad (10)$$

$$\begin{cases} \delta_{\text{opt}} = -2\sqrt{K_{\text{opt}}} \sin\left(\frac{\varphi}{2}\right) = (g_0/2) \tan\left(\frac{\varphi}{2}\right) \\ \sqrt{K}_{\text{opt}} = \frac{(g_0/2)}{\cos(\varphi/2)}. \end{cases} \quad (11)$$

$$(12)$$

It is seen that for low φ , we retrieve $\delta \sim 0$ and $\sqrt{K} = g_0/2$. Also, δ is affected to first order in φ , whereas the coupling \sqrt{K} is affected only to second order. This prescription (11)–(12) can now be used to introduce in a given starting system a detuning to restore a perfect singularity: if the system before correction has $\delta = \delta(g) \neq 0$ at $g = g_0$, we have to add the complementary detuning δ_{corr} :

$$\delta_{\text{corr}} = \delta_{\text{opt}} - \delta(g_0). \quad (13)$$

For small phases, the condition $\sqrt{K} = g_0/2$ is the one from [14]. It is not difficult in the perturbation spirit to adjust the two guides spacers to reach a given modulus of coupling strength \sqrt{K} if we have set their effective indices and know the cladding (spacer) constant $\varepsilon_{\text{clad}}$: we then know what is the spatial law of exponential decay, dictated by $\sqrt{\beta^2 - k_0^2 \varepsilon_{\text{clad}}}$. The quantitative

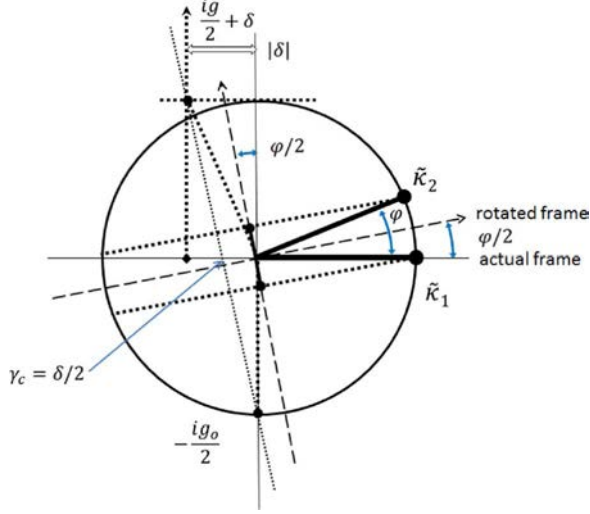


Fig. 4. Graphical interpretation of the detuning correction to restore a complex coupling phase. The matrix coefficients are represented in the complex plane, and a rotated frame is used.

coupling strength can be assessed by the splitting in the absence of gain/loss for instance.

To continue this section, we give a pictorial view of the healing process (see Fig. 4): finding a way to restore a perfect singularity amounts to compensate the phase $\tilde{\kappa}_1 \tilde{\kappa}_2 = K e^{i\varphi}$. We can depict the ideal target matrix just by representing all its four matrix elements m_{jk} of M in the complex plane (not a standard complex plane representation of harmonic quantities): the singularity is known to be perfect for two complex conjugate *nondiagonal terms* and for two purely imaginary *diagonal terms*, one varying ($g/2$) and the other fixed ($-g_0/2$). Since it survives to the addition of any common real constant of the diagonal terms m_{11} and m_{22} , (roots are then complex conjugate rather than lying on real or imaginary axis) we can omit such constant. We now note that this picture of four points can undergo a rotation $e^{i\psi}$, associated with $M e^{i\psi}$, and still produce a singular behavior in the rotated frame, when $g e^{i\psi}$ is varied (at constant ψ). The eigenvalues themselves are also rotated, but importantly, their quadratic evolution around the singular point would be preserved, guaranteeing the essence of PT-enhanced differential gain for reasonable ψ values since the evolution on the complex axis would mostly persist. In this rotated case, the coupling constant product becomes $K e^{i2\psi}$ instead of K .

Conversely, now we have understood that a rotated matrix can work, we may, thus, proceed backward and consider that the nonconjugate *nondiagonal* matrix elements m_{21} and m_{12} of the system to be healed (and thus featuring initially $\tilde{\kappa}_1 \tilde{\kappa}_2 = K e^{i\varphi}$) can just be seen as complex conjugate in a rotated frame (see Fig. 4) built on their bisector $(\tilde{\kappa}_1 + \tilde{\kappa}_2)/2$. This is pictured in a convenient case whereby $\tilde{\kappa}_1$ is real but $\tilde{\kappa}_2$ is complex, without loss of generality (neither does their exact magnitude matter, only their product appears). Thus, if we place the two *diagonal* elements m_{11} and m_{22} correctly in this rotated frame, namely symmetric to the bisector, we are able to reproduce a perfect singularity. Thus, without moving m_{22} , we have to place m_{11} such that at the targeted singular point it is complex conjugate to m_{22} in the rotated frame.

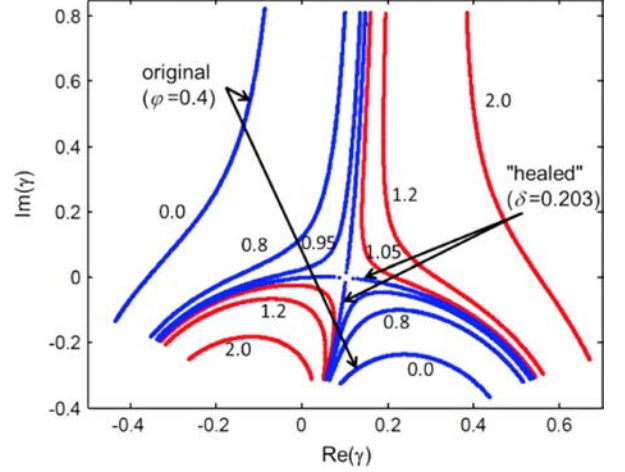


Fig. 5. Trajectories of eigenvalues for $\delta/\delta_c = 0.0, 0.8, 0.95, 1.0$ (blue) 1.05, 1.2, and 2.0 for a case with an original complex coupling phase of 0.4 rad.

As long as with variable gain we travel nearly vertically enough after this singular point, we will produce a nearly optimal form of enhanced differential gain. We, thus, add a small real diagonal term δ that we can guess to be negative. Arranging for a fixed value of δ or for a value that would evolve with g amounts to choose to travel vertically or obliquely, which is of secondary importance. The reader can check that (12) can be drawn from Fig. 4.

Our way to proceed to a “healing” mainly through detuning is dictated by the fact that practically φ cannot be straightforwardly controlled whereas a detuning δ and a given coupling strength K are parameters easy to adjust, respectively, through optogeometric tuning of individual guide section and through guide-to-guide spacing. Thus, we take φ as a quantity imposed by design constraints (specific set of shape and gain/loss region that dictates each isolated mode overlap with the other guide’s gain/loss).

One might now wonder what is the penalty if the requested “healing” conditions are not obeyed. An illustrative sequence is given in the following for the case $g_0 = 1$ and $\varphi = -0.4$ rad, so that $\delta_{\text{opt}} = \delta_{\text{corr}} = -g_0 \tan(\varphi/2) = 0.203$ is the critical detuning to restore the singularity. The diagonal real parts are initially zero for simplicity. The result is given directly in the complex plane in Fig. 5, varying the ratio $\delta/\delta_{\text{opt}}$ across unity, thus, from no correction ($\delta/\delta_{\text{opt}} = 0$) to the nearly symmetrical case of double correction ($\delta/\delta_{\text{opt}} = 2$). The restoration of a perfectly singular point is fully clear. The resulting trajectories, however, now cross at some angle (~ 0.1 rad) instead of the symmetric pattern in Fig. 3(d) in the limit case $\varphi = 0$. This is the trace of the rotation by $\psi = \varphi/2$ combined with the purely imaginary (vertical) trajectory of the guide parameter of the form $(ig/2 + \delta)$. It implies that in a graph versus g , now (as that of Fig. 3(a) for instance), beyond or before the exceptional point, the real parts of the indices in the “healed” case do not describe a single line but rather an acute and “flat” parabola. What also appears is the quadratic trend of the curve around singularity. Thus, without much surprise, if we miss the exact detuning our penalty goes like $(\delta/\delta_{\text{opt}} - 1)^{1/2}$. A similar

rule also holds for the targeted gain, but this was known in the initial cases of Figs. 2 and 3. In general, this makes the procedure somewhat demanding if a high degree of healing is sought. But the aforementioned study of Fig. 3 tells us that the enhanced gain region becomes smoother for imperfect PT symmetry with a remaining phase, which is practically a welcome situation to operate under relaxed absolute gain conditions and ensuring a smaller but more easily reproducible enhancement.

IV. EXACT EXAMPLES FOR PLANAR AND CHANNEL WAVEGUIDES

A. Dielectric-Based Waveguides

We now compare these predictions modeled with the sole CMT to those of actual guides, accounted with exact electromagnetism, at a given frequency. The simplest case is a 1-D geometry $\varepsilon = \varepsilon(x)$, namely a stack of different layers out of which two are guiding, one with some fixed loss and the other with a variable gain.

For such a 1-D stack, it suffices to set dielectric constants and to give dimensionless thicknesses of the j th layer in the form $\bar{d}_j = \text{thickness} \times 2\pi/\lambda$ to take advantage of scaling laws. Numerically, to hunt for complex poles in complex $z \equiv n_{\text{eff}}$ space ($k_{z/j} = 2\pi/\lambda n_{\text{eff}}$ can also be used), we found it convenient to use the noniterative Cauchy integrals of the complex analytical diverging quantity of the transfer matrix T of the system [23], typically $f(z) = 1/T_{22}$: we have

$$(n_{\text{eff}})_{\text{pole}} \equiv z_{\text{pole}} = \frac{\oint z f(z) dz}{\oint f(z) dz}. \quad (14)$$

If a single pole is in the contour, the residue simplifies. Here, we used two to four half-circles to safely get the poles with minimal algorithmic effort.

In our first example (see the inset of Fig. 6), both waveguides WG1 and WG2 have a constant $\varepsilon = 4 + i\varepsilon''$ and a width $\bar{d}_2 = \bar{d}_4 = 2$ (this corresponds, say, to silicon nitride at $\lambda = 1 \mu\text{m}$ and thickness $\sim 320 \text{ nm}$). The cladding (i.e., layers 1, 3, 5 with obvious numbering) has a constant $\varepsilon = 2.25 = 1.5^2$ (say, silica or polymer). For the time being, WG1 is uniformly lossy with $\varepsilon = 4 - 0.1i$, whereas the variable gain-carrying WG2 guide features localized gain in the form $\varepsilon = \varepsilon'_4 + i\varepsilon''_4 = 4 + i\varepsilon''_4$ only in its central half of thickness $\bar{d} = 1$, the two sides of thickness $\bar{d} = 0.5$ being gain free. From the study of the isolated guides, we get their gain/losses in terms of $\text{Im}(n_{\text{eff}})$, and we can also access the relevant partial derivatives $\partial \text{Im}(n_{\text{eff}})/\partial \varepsilon'_4$ and $\partial \text{Re}(n_{\text{eff}})/\partial \varepsilon'_4$, so that we control gain and detuning through these handles. From the knowledge of the loss of WG1 $g_0 = 2 \text{Im}(n_{\text{eff}})$, and from the calculation of the splitting of WG1 and WG2 for any cladding layer spacing \bar{d}_3 first guess, we can restore the situation of [14], $\sqrt{K} = g_0/2$: we get the coupling strength for any thickness, say $\bar{d}_3 = 2$, and we infer the way to reach this condition from the fact that for given effective indices, the coupling strength \sqrt{K} has the well-known behavior dictated by the decay constant $(2\pi/\lambda)(\varepsilon - n_{\text{eff}}^2)^{1/2}$. Here, we arrive at $\bar{d}_3 = 1.6796$.

The use of the aforementioned analysis on the eigenvalues (poles) of the system with optimal $\bar{d}_3 = 1.6796$

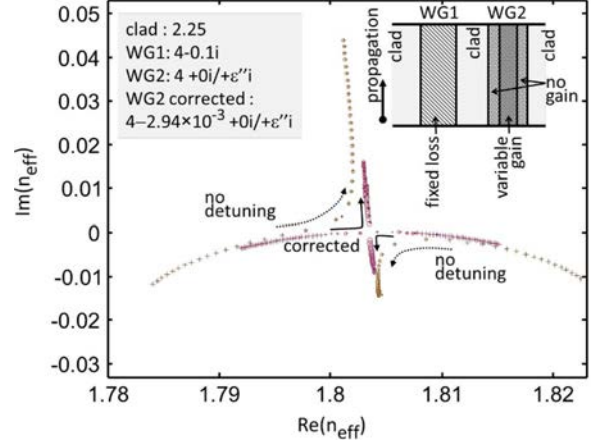


Fig. 6. Trajectory of the complex indices for the coupled-waveguide system, not detuned and detuned (“corrected”) with the correction that restores the singularity. The points correspond to a scan in ε''_4 , with a coarser graining in the no detuning case than in the corrected case, by a factor of 4.

confirmed us that the coupling strength K is pretty constant ($K = 4.77 \cdot 10^{-4}$), whereas the phase φ evolves much more. In this particular case, it turns out to change sign from positive to negative upon the increase of ε''_4 . Given the sharper gain repartition in the gain-carrying WG2 waveguide, the gain/loss equality $g = g_0$ is attained for $\varepsilon''_4 \approx 0.17$. At this point, our correction yields a phase $\varphi = -0.0245$. The correction $\delta_{\text{corr}} = \delta_{\text{opt}} - \delta(g_0)$ then decomposes into $\delta_{\text{corr}} = (4.3 \cdot 10^{-4} - (-2.24 \cdot 10^{-4})) = 6.54 \cdot 10^{-4}$. Eventually, making use of $\partial \text{Re}(n_{\text{eff}})/\partial \varepsilon'_4 = 4.568^{-1}$, we get the detuning correction to be made on our WG2: we have to increase its dielectric constant by $\Delta \varepsilon'_4 = 2.98 \cdot 10^{-3}$. This is a typical value of electro-optic material and devices, by the way. At the present stage, only the high gain ($\varepsilon = 4 + 0.17i$) is not clearly realistic today, but we have discussed this point in [14].

Fig. 6 presents the two complex trajectories of eigenvalues n_{eff} : the one before healing and the one for the “healed” case.

B. Phase of Coupling

We next consider a case where the role of the phase versus the optogeometric parameters is more significant than the aforementioned case: we now localize the fixed losses in either the “far” or the “close” half of WG1. All the rest of the study is the same, the ε'_4 values being just twice larger because the overlap of the guided mode with the gain region exists only in one half. We note in Fig. 7 that the initial cases have different phase signs around the crossing, with similar absolute values, leading to opposite trends at the avoided crossing. Nevertheless, the healing strategy works well. The final tilt of the exceptional point crossing thus is seen to depend logically on the optogeometric parameters. In the “far” case, the complex gain is less than what the real part coupling involves, and conversely in the “close” case, it is more, leading to distinct complex coupling behaviors, which in turn request distinct corrective angles of rotation ψ . Only one coupling constant is affected by the change (mode of WG2 \rightarrow loss of WG1) not the other one, so we do not have the most heuristic situation which would be opposite rotation angles.

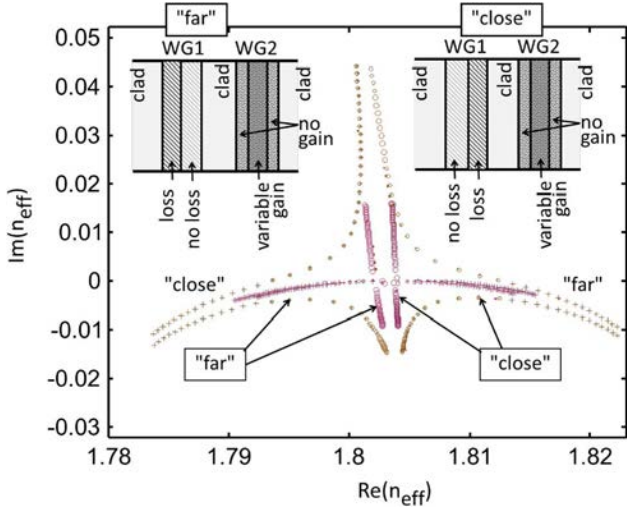


Fig. 7. Same as in Fig. 6, except that losses are now localized either “far” or “close” from the gain-carrying waveguide. Both data are superimposed and designed by arrows. Note the distinct patterns of the original cases and the remaining difference in tilt angle on approaching the exceptional point between the two “corrected” cases.

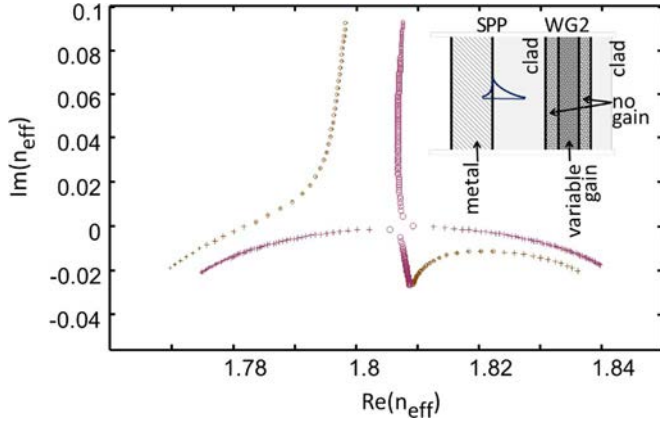


Fig. 8. Plasmonic case: eigenvalues in the case of a dielectric waveguide with variable gain and core real index $n = 2$ as in Fig. 7, coupled to a SPP supported by a fictitious metal ($\epsilon = -7.187 - 0.7i$). The starting configuration has a large avoidance of the singularity (smaller crosses and circles); the corrected one (core dielectric constant shift of $\delta\epsilon = 0.0396$), more densely sampled here, is nearly perfect (larger crosses and circles).

C. Surface Plasmon Polariton

As a final 1-D example, we study a plasmonic case for the loss-carrying guide, thus in the TM polarization in 1-D [17]. The stack consists of a formal ad hoc “metal” ($\epsilon = -7.187 - 0.7i$) supporting a surface plasmon polariton (SPP), a low index spacer ($n = 1.5 \dots$), and a high index guide ($n = 2$) comprising a central gain region as in Fig. 7 case. The phase is found to be $\varphi = -0.225$ rad and the detuning correction is predicted to be $\delta = 0.00867$ in terms of effective index, requiring a core dielectric constant shift of $\delta\epsilon = 0.0396$, about 1%. The result compared to the original situation is very satisfying (see Fig. 8), showing that the nature of the loss channel (more dielectric or more fully metallic) is indifferent.

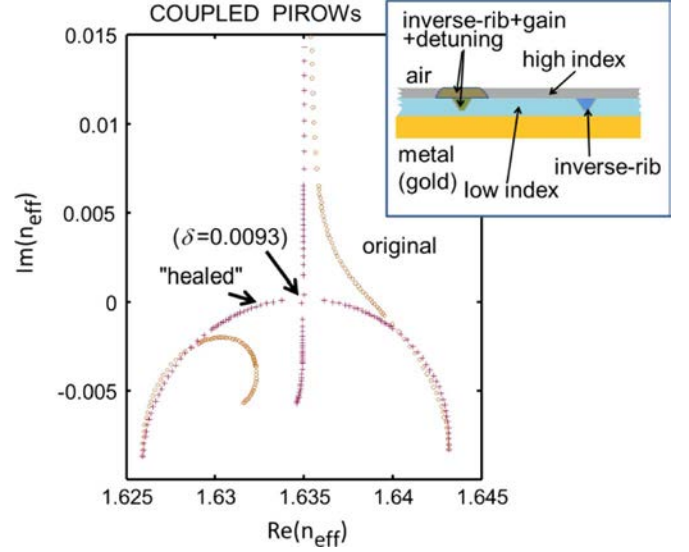


Fig. 9. Eigenvalue trajectories for original coupled PIROW structured and “healed” PIROW structure.

D. Coupled Inverse-Rib Plasmonic Waveguides

We now detail a first 2-D example, a study made by trial and error [12]. The basic waveguides belong to the family of the so-called hybrid waveguide making use of a high-index/low-index/metal sandwich, and allowing strongly subwavelength mode sizes if the low-index gap is of small dimensions in both transverse directions. The first initial study [19], [20] dealt with cylindrical high-index systems and led to the first longitudinal “spaser” [18]. We proposed a technologically simple and deterministic way to get similar situations, the so-called plasmonic inverse-rib optical waveguide (PIROW) whereby a high index planarization of a grooved low index resist on a flat metal achieves essentially the same result. A starting point is [22, Fig. 1] for PIROW definition, and then [14, Figs. 5 and 6] for a first example of coupled passive PIROW structures. In [12, Fig. 9], we empirically found that detuning did restore the singularity. Here, we apply the aforementioned analysis to check the relevance of our approach in deterministically providing the detuning correction. The results of [12] are plotted in Fig. 9 in the complex plane. The quantity scanned is the gain of the inverse rib together with the gain of the fraction of the top high-index slab indicated in the inset, to compensate the plasmonic losses with less material gain than if in the rib only. Corrective detuning is supposed to be implemented only in this top fraction, which adds some complexity, but also exemplifies the robustness of our approach.

The analysis indicates again that K is nearly constant, but here the phase is relatively large ($\varphi = -0.097$ rad) as could be expected from the broadly avoided singularity in the original case. The detuning correction in terms of effective index is 0.00164, which corresponds here to add a positive index shift in the top part of the PIROW of about 0.010. The empirical choice was 0.0092, hence an 8% discrepancy. We hypothesize that this might stem from the complex situation denoted previously, with both waveguides carrying losses, even the gain one.

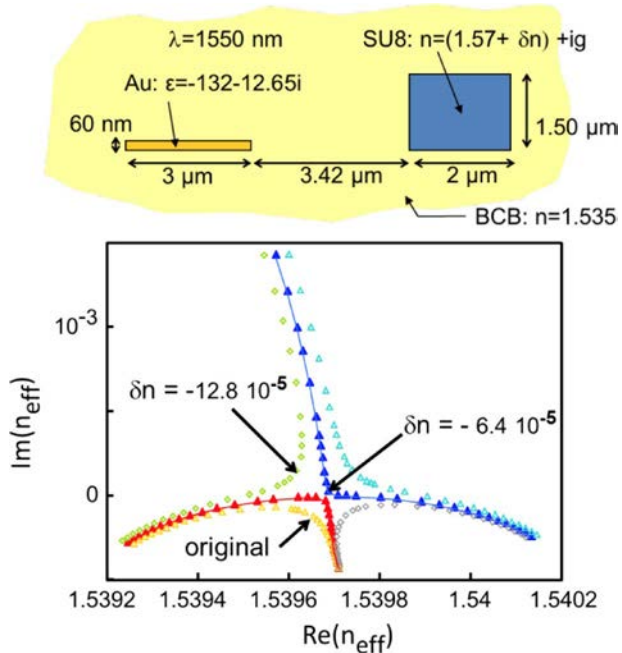


Fig. 10. Eigenvalue trajectories for coupled LRSPP waveguide and SU8 (high-index polymer) waveguides in polymer (BCB) in three cases for a wavelength $\lambda = 1550$ nm: tuned at zero gain (“original” $\delta n = 0$, yellow and light blue triangles), corrected to restore the singularity ($\delta n = -6.4 \cdot 10^{-5}$, red and blue triangles) and “over-corrected” ($\delta n = -12.8 \cdot 10^{-5}$, green and gray diamonds). The inset depicts the geometry in question, with the LRSPP guide on the left and the dielectric guide on the right.

E. LRSPP

We finish these examples by the case of a LRSPP channel waveguide coupled to low-index-contrast channel waveguide [21], in which modes are rather “deconfined,” and polarization is quasi TM, i.e., vertical in the inset of Fig. 10. Here, the same procedure is applied we track individual guide properties, then get to a zero detuning situation associated with the proper coupling $\sqrt{K} = g_0/2$ given the LRSPP guide losses, and finally we apply the correction through a higher index in the SU8 core than originally. Here, the coupling requirement $\sqrt{K} = g_0/2$ translates into a large $3.42 \mu\text{m}$ spacing between the guides given the weak losses. The extra index contribution needed to restore the singularity is in the $\delta n \sim 10^{-4}$ range, e.g., accessible by thermo-optical tuning. Actually, compared to the empirical value $\delta n = -6.410 \cdot 10^{-5}$, our correction approach (characterized by $\varphi = 13.1$ mrad only) yields a nearly perfect result $\delta n = -6.3810 \cdot 10^{-5}$ (a shift of $-2.46 \cdot 10^{-5}$ in n_{eff}). Such a good agreement is at variance with the slight discrepancy of the double PIROW case above. These distinct behaviors are in support of our assumptions for the complexity of this double PIROW case, notably the presence of losses in both guides.

V. CONCLUSION

The concept of PT-symmetry breaking brings, beyond its fundamental interest, the opportunity to implement a high differential gain near its exceptional point, and furthermore to do this by interaction of the gain system with a loss-carrying waveguide. Such a situation may notably include a plasmonic or

metal-based waveguide [14] in conjunction with a more standard dielectric waveguide for instance. To date only so-called passive PT-symmetric structures, with only losses and no gain, have been studied [8] with metals. Other PT-symmetric realizations involve more peculiar gain regimes [11].

We have first outlined how much differential gain would be available. This crucially depends on the degree of perfection of the PT-symmetry breaking. A critical control parameter of this perfection is the phase of the product of the coupling constants $\tilde{\kappa}_1 \tilde{\kappa}_2 = K e^{i\varphi}$. This phase is responsible for smoothing the singularity; it has a physical basis and is not dependent on any “phase origin”; only individual coefficient may have such a dependence. The smoothing of eigenvalue evolution close to the exceptional point is initially slightly beneficial in the sense that it avoids a divergence of the differential gain near the singularity, but this smoothing can rapidly become detrimental to the very existence of a decent differential gain. We have made this scenario more quantitative.

We have then given an account of PT-symmetric coupled waveguide systems in the framework of coupled mode theory to explain why and how the presence of this detrimental phase could be “healed” to restore a genuine singular behavior versus the gain of the active waveguide. This involves simply a detuning of the two waveguides, which was explained graphically as well in Fig. 4. This had been made only by trial and error in a first case, and is now confirmed by an examination of the coupled-mode-theory results.

We have eventually applied this approach to heal a number of waveguide systems, either of the slab or of the channel type. We start from a tuned system, whose individual effective indices are known (a constant loss-carrying waveguide and a variable gain waveguide), as well as their tuning characteristic, i.e., the coefficients (partial derivative) which tell how one of the constituent dielectric constant influences the real part of their effective index. We then check that the detuning predicted from the coupled mode theory does restore the singularity nearly entirely. A few slab systems were used as models to point out what are the handles liable to influence the coupling phase in question, including a SPP case. Channel waveguide cases were intended to be more realistic. One of them is the PIROW case used for the trial-and-error first account [12], while the other is the LRSPP + SU8 system embedded in SU8, for which experimental proof of the coupling behavior is among the best characterized to date [21].

We have, thus, provided tools to make good use of the PT-symmetry breaking singularity to produce high differential gains in real-life systems, and hope to test these effects in experiments.

REFERENCES

- [1] Y. D. Chong, L. Ge, and A. D. Stone, “PT-symmetry breaking and laser-absorber modes in optical scattering systems,” *Phys. Rev. Lett.*, vol. 106, p. 093902, 2011.
- [2] J. Ctyroky, V. Kuzmiak, and S. Eyderman, “Waveguide structures with antisymmetric gain/loss profile,” *Opt. Express*, vol. 18, pp. 21585–21593, 2010.
- [3] S. Longhi, “PT-symmetric laser absorber,” *Phys. Rev. A*, vol. 82, Sep. 2010.
- [4] H. P. Nolting, G. Sztefka, M. Grawert, and J. Ctyroky, “Wave propagation in a waveguide with a balance of gain and loss,” in *Proc. Integr. Photon. Conf.*, Boston, 1996, p. IMD5-1.

- [5] J. Ctyroky, S. Helfert, R. Pregla, P. Bienstman, R. Baets, R. De Ridder, R. Stoffer, G. Klaasse, J. Petracek, P. Lalanne, J. P. Hugonin, and R. M. De La Rue, "Bragg waveguide grating as a 1D photonic band gap structure: COST 268 modelling task," *Opt. Quant. Electron.*, vol. 34, pp. 455–470, May–Jun. 2002.
- [6] M. Kulishov, J. M. Laniel, N. Bélanger, J. Azaña, and D. V. Plant, "Nonreciprocal waveguide Bragg gratings," *Opt. Express*, vol. 13, pp. 3068–3078, 2005.
- [7] M. Kulishov, J. M. Laniel, N. Bélanger, and D. V. Plant, "Trapping light in a ring resonator using a grating-assisted coupler with asymmetric transmission," *Opt. Express*, vol. 13, pp. 3567–3578, 2005.
- [8] A. Guo, G. J. Salamo, R. Duchesne, R. Morandotti, M. Volatier-Ravat, V. Aimez, G. A. Siviloglou, and D. N. Christodoulides, "Observation of PT-symmetry breaking in complex optical potentials," *Phys. Rev. Lett.*, vol. 103, p. 093902, 2009.
- [9] S. Klainman, U. Günther, and N. Moiseyev, "Visualization of branch points in PT-symmetric waveguides," *Phys. Rev. Lett.*, vol. 101, p. 080402, 2008.
- [10] T. Kottos, "Broken symmetry makes light work," *Nat. Phys.*, vol. 6, pp. 166–167, 2010.
- [11] C. E. Rüter, K. G. Makris, R. El-Gaininy, D. N. Christodoulides, M. Segev, and D. Kip, "Observation of parity-time symmetry in optics," *Nat. Phys.*, vol. 6, pp. 192–195, Jan. 2010.
- [12] H. Benisty and M. Besbes, "Confinement and optical properties of the plasmonic inverse-rib waveguide," *J. Opt. Soc. Amer. B*, vol. 29, pp. 818–826, Mar. 2012.
- [13] G. W. Ford and W. H. Weber, "Electromagnetic interaction of molecules with metal surfaces," *Phys. Rep.*, vol. 113, pp. 195–287, 1984.
- [14] H. Benisty, A. Degiron, A. Lupu, A. De Lustrac, S. Chenais, S. Forget, M. Besbes, G. Barbillion, A. Bruyant, S. Blaize, and G. Lerondel, "Implementation of PT symmetric devices using plasmonics: Principle and applications," *Opt. Express*, vol. 19, pp. 18004–18019, Sep. 2011.
- [15] I. De Leon and P. Berini, "Amplification of long-range surface plasmons by a dipolar gain medium," *Nat. Photon.*, vol. 4, pp. 382–387, 2010.
- [16] M. C. Gather, K. Meerholz, N. Danz, and K. Leosson, "Net optical gain in a plasmonic waveguide embedded in a fluorescent polymer," *Nat. Photon.*, vol. 4, pp. 457–461, 2010.
- [17] M. A. Noginov, V. A. Podolskiy, G. Zhul, M. Mayyl, M. Bahoural, J. A. Adegoke, B. A. Ritzo, and K. Reynolds, "Compensation of loss in propagating surface plasmon polariton by gain in adjacent dielectric medium," *Opt. Express*, vol. 16, pp. 1385–1392, 2008.
- [18] R. F. Oulton, V. J. Sorger, T. Zentgraf, R.-M. MA, C. Gladden, L. Dai, G. Bartal, and X. Zhang, "Plasmon lasers at deep subwavelength scale," *Nature*, vol. 461, pp. 629–632, 2009.
- [19] R. F. Oulton, G. Bartal, D. F. P. Pile, and X. Zhang, "Confinement and propagation characteristics of subwavelength plasmonic modes," *New J. Phys.*, vol. 10, p. 105018, Oct. 2008.
- [20] R. F. Oulton, V. J. Sorger, D. A. Genov, D. F. P. Pile, and X. Zhang, "A hybrid plasmonic waveguide for subwavelength confinement and long-range propagation," *Nat. Photon.*, vol. 2, pp. 496–500, July 2008.
- [21] A. Degiron, S. Y. Cho, T. Tyler, N. M. Jokerst, and D. R. Smith, "Directional coupling between dielectric and long-range plasmon waveguides," *New J. Phys.*, vol. 11, pp. 01500201–01500210, 2009.
- [22] H. Benisty and M. Besbes, "Plasmonic inverse rib waveguiding for tight confinement and smooth interface definition," *J. Appl. Phys.*, vol. 108, pp. 0631081–0631088, 2010.
- [23] D. Felbacq, "Finding resonance poles by means of Cauchy integrals," in *Proc. 13th Int. Conf. Transp. Opt. Netw.*, Stockholm, 2011, p. 4.